Presented at the 29th European PV Solar Energy Conference and Exhibition, 22-26 September 2014, Amsterdam, The Netherlands

THE INFLUENCE OF THE ADDITIVE COMPOSITION ON DEGRADATION INDUCED CHANGES IN POLY(ETHYLENE-CO-VINYL ACETATE) DURING PHOTOCHEMICAL AGING

Angelika Beinert[1], Cornelia Peike[1], Ines Dürr[1], Michael D. Kempe[2], Günter Reiter[3], Karl-Anders Weiß[1]
[1]Fraunhofer Institute for Solar Energy Systems (ISE)
Heidenhofstraße 2, D-79110 Freiburg, Germany
[2]National Renewable Energy Laboratory
15013 Denver West Parkway, Golden, Colorado
[3]Institute of Physics，Albert-Ludwigs-University of Freiburg
Hermann-Herder-Str. 3, 79104 Freiburg, Germany

ABSTRACT: Comprehensive knowledge about the influence of the additive composition on the degradation behavior of the most important photovoltaic (PV) module encapsulant, ethylene vinyl actetate (EVA), is crucial for enhancing its durability. To analyze this influence, EVA foils with different additive compositions were exposed to UV irradiation (135 W/m^2) at 60 °C with a UV-A lamp, and characterized by spectroscopic methods (UV-vis, Raman spectroscopy) and DSC measurements. The reference foil with minimal additives showed significant changes in consistency during UV exposure. Those changes were explained by chain scissions, changes in conformation and crystallinity. In particular, degradation induced changes in the intensity of the symmetric compared to the asymmetric CH_2 stretching vibrations, detected by Raman spectroscopy, indicate modifications in the conformational and crystalline setup. Therefore, their intensity ratio offers a nondestructive method to follow EVA degradation in PV modules. A major influence of additives on the development of fluorescent and chromophoric species was found. A quenching effect of oxygen on the development of fluorescent species was observed.

Keywords: Ethylene-vinyl acetate, degradation, nondestructive investigation, Raman spectroscopy

1 INTRODUCTION

Ethylene vinyl acetate (EVA) is the most commonly used cell encapsulant in c-Si-PV modules. EVA is a semi-crystalline copolymer composed of Polyethylene (PE) and Vinyl acetate (VA). The PE chains are partly folded to crystals, that form reversible physical crosslinks in the polymer network. Irreversible chemical crosslinks are built during the module lamination process above 140 °C. Through the peroxidic crosslinking process EVA becomes an elastomer with high elasticity and a low elasticity modulus. Therefore EVA can reversibly transform deformations ε in low stresses σ (σ=ε*E), which is an important function of a module encapsulant.
Environmental influences like oxygen, UV irradiation and high temperatures induce EVA degradation. Degradation influences the optical and mechanical properties of EVA depending on its route. Under the influence of irradiation, EVA mainly degrades via Norrish reactions, that result in deacetylation of the EVA chains as well as ketone, aldehyde, acetic acid and radical formation.[1], [2] Radicals introduce chain scission as well as crosslinking. It has been found, that the influence of oxygen in particular leads to chain scission. [2] Additionally EVA degradation is usually accompanied by the generation of fluorescent species.
Stabilizing additives like UV absorber, antioxidants or hindered amine light stabilizers (HALS) affect different steps of the degradation process Therefore it is possible that they influence the degradation route. They can interact synergistically or antagonistically. It is the purpose of this work to achieve a more fundamental knowledge about specific stabilizer interactions as well as the degradation process and investigation methods.

EVA foils with different additive compositions were exposed to UV irradiation (135 W/m^2) at 60 °C using a UV-A lamp. Their degradation behavior was investigated by UV-vis-, Raman- and DSC measurements. Hemispherical UV-vis transmission measurements provide information about degradation induced changes in solar transmittance and UV absorber efficiency. Raman spectroscopy was applied as a non-destructive characterization method to track changes in the chemical, crystalline and conformational structure of the foils. DSC measurements were conducted to gain a deeper understanding of the changes in the crystallinity. A special focus was also set on the potential of Raman as a nondestructive testing method.

2 MATERIALS AND TECHNIQUES

2.1 Sample preparation and aging process

Table 1: The investigated additive compositions: Values in parts per hundred rubber (phr).

Function	Name	#1	#2	#9	#9	#10
EVA	Elvax® 1400	100 phr for all compositions				
Crosslinking Agent	TBEC	1,50	1,50	1,50	1,50	1,50
Antioxidant.	Irgafos 168			0,25		
UV-Abs.	Tinuvin 234		0,30	0,30	0,30	
UV-Abs.	Cyasorb 531					0,3
NOR-HALS	Tinuvin 123		0,13			
HALS	Tinuvin 770		0,13		0,13	0,13
Coupling agent	Dow Corning Z6030		1,20	1,20	1,20	1,20

EVA foils based on Elvax® 1400 with five different stabilizer compositions (Table 1) were designed and extruded at the National Renewable Energy Research Laboratory (NREL, USA). Elvax® 1400 has a VA content of 33 wt%. The raw Elvax 1400 pellets had about 0.055 phr of butylated hydroxytoluene (BHT), a phenolic antioxidant, from the manufacturer which was not removed prior to formulation.
The foils were cured in a Meier vacuum laminator ICOLAM 10/08. They were exposed to UV irradiation (UV-A: 135 W/m^2, UV-B: 1 W/m^2) at 60°C sample temperature for a total dose of 470 kWh/m^2 in a Horstmann HS 220 K45 L climatic chamber.

Spectroscopic measurements were conducted every 20-50 kWh/m^2. Samples consisted of bare foils about 0.45 mm thick.

2.2 UV-vis-spectroscopy

UV-vis hemispherical transmission measurements were conducted by a customized Vertex70 from Bruker. Per measurement a total of 128 spectra were averaged. The solar transmittance (AM1,5) was determined from the spectra. The absolute error of the Solar Transmittance is 1 %, but the relative error lies below 0,5 %.

2.3 Raman spectroscopy

Raman measurements were carried out by a WITec alpha 500. It provides a confocal setup, which makes it possible to measure in one focal plane. The measurements were taken on the sample surface. For one measurement three spectra with an integration time of 20 s were recorded and averaged. Per aging step, three measurements were taken at different positions on the sample surface and averaged. Spectral resolution is 3 cm^{-1}.

2.4 DSC measurements

DSC measurements were carried out with a Q200 from TA Instruments. The heating rate was 10 K/min. Two cycles were recorded between -80 °C and 200 °C under a nitrogen flow of 50 ml/min. The sample weight varied between 7 mg and 10 mg. The heat flow was weighted by the sample weight.

3 RESULTS

3.1 Visual changes

The sample without additional stabilizing additives, beyond the BHT in the EVA pellets, (#1 in Table 1) became gradually tenacious and semifluid between 83 kWh/m^2 and 117 kWh/m^2 at 60 °C (Figure 1 left picture). Between 270 kWh/m^2 and 312 kWh/m^2 it hardened and cracks were clearly visible (Figure 1 right picture). The sample remained clear until a total dosis of 312 kWh/m^2, where severe discoloration was observed. All other samples showed almost no visible changes.

Figure 1: Left: EVA sample 1 became semifluid and tenacious after 117 kWh/m^2 at 60 °C. Right: After 312 kWh/m^2 the sample hardened and cracks are visible.

3.2 Raman Spectroscopy

Figure 2 shows the Raman spectrum of a typical EVA. For this study in particular the CH_2-scissoring vibrations at 1416 cm^{-1}and 1440 cm^{-1}, the CH_2 stretching vibrations at 2832 cm^{-1} and 2913 cm^{-1}and the Carbonyl vibration (C=O) at 1735 cm^{-1} were investigated. The Carbonyl peak results from the Vinyl acetate groups.

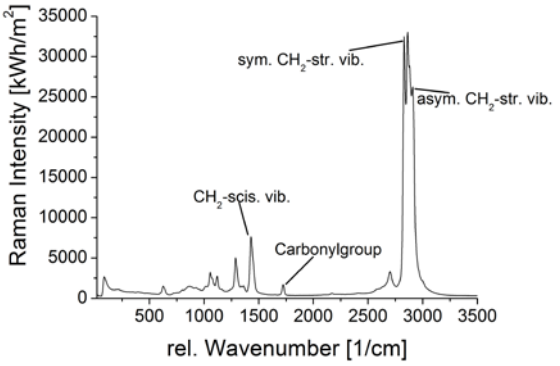

Figure 2: Representative Raman spectrum of EVA

3.2.1 Deacetylation

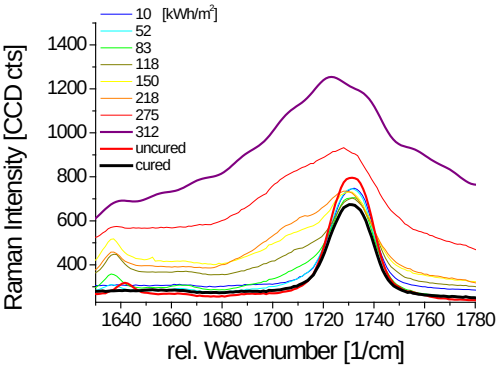

Figure 3: The Raman spectrum of the carbonylpeak at 1735 cm^{-1} of sample 1 in the course of aging. ”Cured” and ”Uncured” are not aged. The fluorescense background increases during aging.

Figure 3 shows the Raman spectra of sample 1 around the carbonyl peak at 1730 cm^{-1} during the aging process. The carbonyl peak of sample 1 is broadening during the aging process. The shoulder at 1710 cm^{-1} most likely results from degradation induced ketone formation in the backbone resulting from deactylation, and the shoulder at 1760 cm^{-1} results from lactone formation.[2]

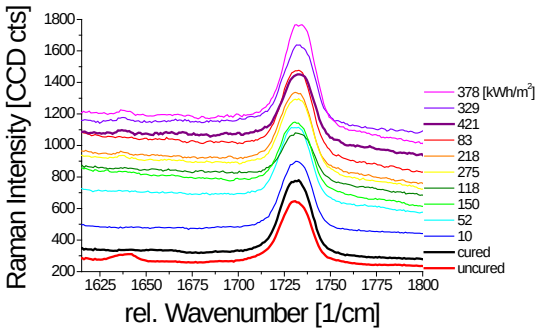

Figure 4: The Raman spectrum of carbonylpeak at 1735 cm^{-1} for sample 9 in the course of aging.

Figure 4 shows this region for sample 9. The other samples with both UV absorber and HALS based stabilizers show a similar behavior like sample 9. The samples with stabilizers do not show any broadening of the carbonyl peak, indicating a lack of significant deactylation. The higher fluorescence background upon aging is significant for the samples with stabilizers and will be discussed in 3.2.2. .

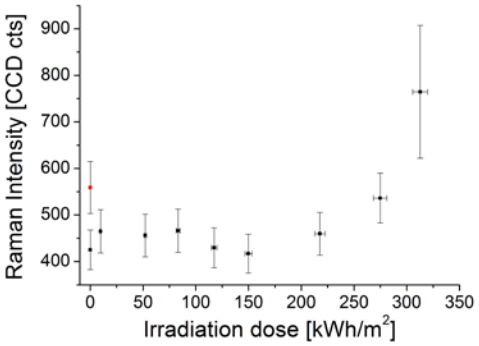

Figure 5: The development of the Raman intensity of the carbonyl peak during aging in sample 1.

As can be seen in Figure 5, the carbonyl peak intensity of sample 1 is increasing. This could result from an increase of carbonyl groups at the chain ends due to chain scission.[2] The intensity of the samples with stabilizers shows no significant trend for changes of the carbonyl peak intensity within the error. The carbonyl peak intensity of the uncured sample 1 (Figure 5 red point at 0 kWh/m^2) is higher than the intensity of the cured sample 1 (Figure 5 black point at 0 kWh/m^2). This can possibly be explained by crosslinking reactions via the carbonyl groups, which lead to a reduced number of carbonyl groups. For the samples with stabilizers the same trend can be observed after the subtraction of the fluorescence background. But it is not confirmed within the error.

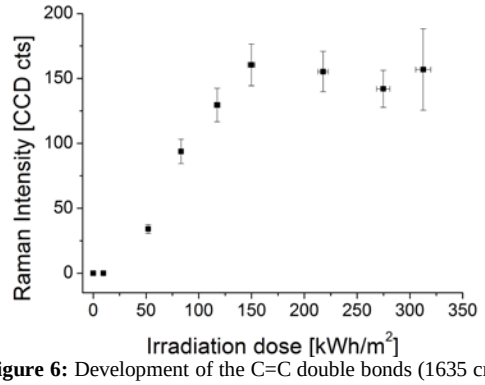

Figure 6: Development of the C=C double bonds (1635 cm^{-1}) in sample 1 during aging.

Furthermore a peak at 1635 cm^{-1} was developed during aging in the spectrum of sample 1 from 50 kWh/m^2 on. (Figure 6). The samples with added stabilizers show a peak development of this peak from 220 kWh/m^2 on. The intensity is too small to be numerically determined. The peak presumably derives from C=C double bonds, which are an indication of double-bond formation via deactylation (Norrish II reaction).[3, 4] From 125 kWh/m^2 on the development of C=C double bonds remains at the same level. This could be the result of photooxidation, which leads to the degradation of previously formed double bonds (photobleaching).[1]
All the non-crosslinked samples show a peak at 1640cm^{-1}. It could derive from C=O bonds of the curing agent, which would explain, that the peaks are vanished after crosslinking.

3.2.2 Development of fluorescent species

Fluorescent species lead to a spectral underground. The origin of fluorescent species is still a topic of scientific discussion. It is assumed, that it is partly correlated with the development of chromophoric species deriving from the additives.[4]
To represent the development of the fluorescent species the Raman spectra are integrated between 1900 cm^{-1} and 2400 cm^{-1}. This area was chosen, because no peaks appear in the spectrum within this range. The resulting values are shown in Figure 7.

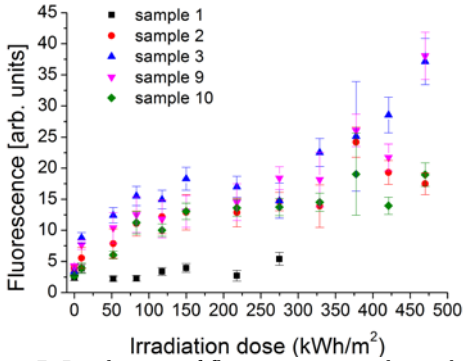

Figure 7: Development of fluorescent species during the aging process. It is represented by the integrated area from 1900 cm^{-1} – 2400 cm^{-1}

Compared to sample 1, the samples with added stabilizers develop a significantly higher amount of fluorescent species. This indicates that the development of fluorescent species is influenced by the added stabilizers. It is possibly correlated to the development of chromophoric species, which is well known to be enhanced by additive interactions.[1, 4]
Sample 3 and sample 9 (same stabilizer composition with the exception of Irgafos 168 (sample 3)) establish a higher amount of fluorescent species than sample 2 and sample 10. This could result from the combination of Tinuvin 234 (UV-absorber) and Tinuvin 770 (HALS), which differ from the other samples. The presence of these two stabilizers is correlated with higher fluorescence.
Furthermore the development of fluorescent species was less pronounced than for foils aged in a glass-EVA-glass setup with the same stabilizer composition.[5] Therefore it is assumed that oxygen has a quenching effect on the development of fluorescent species. Similar observations have been made before in particular with regard to yellowing.[1]

3.2.3 Changes in crystallinity

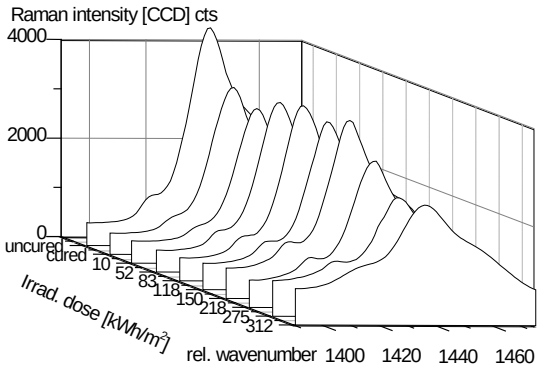

Figure 8: Raman spectrum of the CH_2 scissoring vibrations around 1440 cm^{-1} for sample 1. The shoulder at 1416 cm^{-1} develops during aging whereas the intensity of the other peaks decreases.

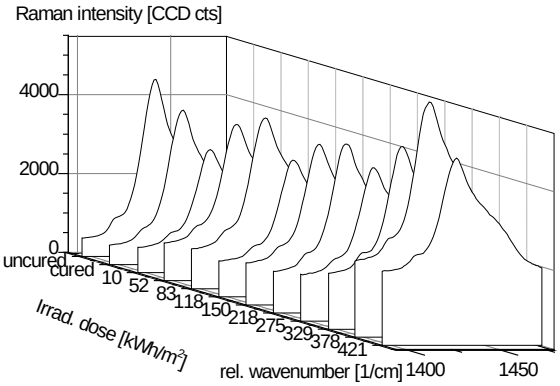

Figure 9: The Raman spectrum of the CH_2 scissoring vibrations around 1440 cm^{-1} for sample 3.

Figure 8 and Figure 9 show the Raman spectra of the CH_2 scissoring vibrations around 1440 cm^{-1} for sample 1 and exemplary for the samples with stabilizers for sample 3. For all samples the intensity of the peak at 1440 cm^{-1} decreases after crosslinking. For sample 1 it also decreases during aging compared to the increasing fluorescence background. A decrease in peak intensity after crosslinking and during aging applies also to all investigated polyethylene related peaks in the Raman spectrum of sample 1 (see also Figure 11). The reason for this is not fully understood, yet. It is possible that a minimum chain length is required for the chains to be Raman-active.[6] Both chain scission and crosslinking reduce the free chain lengths. Both processes can take place simultaneously during degradation. A higher rate of chain scission would explain the liquefaction of sample 1, whereas a higher rate of radical induced crosslinking could have induced the observed hardening.

Compared to the decreasing intensity of the peak at 1440 cm^{-1} it is significant, that the intensity of the shoulder at 1416 cm^{-1} (also a CH_2-scissoring vibration) is increasing for sample 1 (Figure 10). For the samples with additional added stabilizers it is not possible to determine the effect within error boundaries.

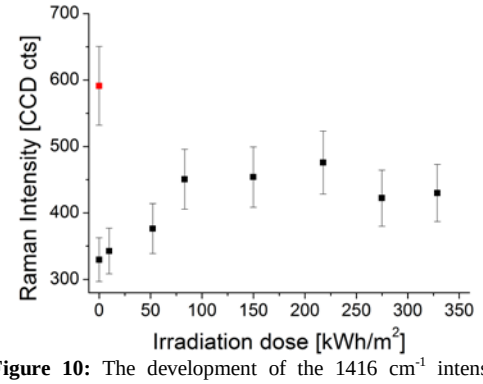

Figure 10: The development of the 1416 cm^{-1} intensity for sample 1 during aging. The red point ist the uncured sample.

The shoulder at 1416 cm^{-1} results from crystal unit cells. The crystal unit cell contains two PE units, which lead to in-phase and anti-phase vibrations respectively the 1416 cm^{-1} and 1440 cm^{-1} scissoring vibrations.[7] For less organized crystals only the 1440 cm^{-1} vibration appears. Therefore the increasing intensity of the shoulder at 1416 cm^{-1} could indicate a relative increase of better organized crystals during aging.

For all samples the 1416 cm^{-1} intensity before crosslinking is higher than after (for sample 1: red point Figure 10). The crosslinks most likely disturb the folding of better organized crystals. Additionally the decrease after crosslinking might also result from the reduction of Raman-active chain lengths due to crosslinking.

It is important to note, that the intensity of 1416 cm^{-1} is only an indication for the increase of highly organized crystals and not for an increase in the total amount of crystalline phase. In fact the total amount of crystals might decrease (will be discussed in 3.2.4). To further confirm the relative increase of better organized crystals DSC measurements were carried out (discussed in 2.4).

3.2.4 Conformational changes

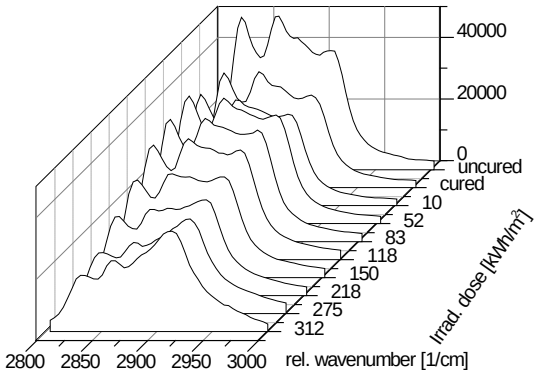

Figure 11: The development of CH_2-stretching vibration of sample 1 during aging.

Figure 11 shows the symmetric and asymmetric CH_2 stretching vibrations (2832 cm^{-1} and 2913 cm^{-1}.) and the CH_3 (2861 cm^{-1}) of sample 1 during aging. The ratio of the asymmetric to the symmetric stretching vibration increases approximately exponentially for sample 1. The ratio shows no significant changes for the samples with additional added stabilizers (Figure 12).

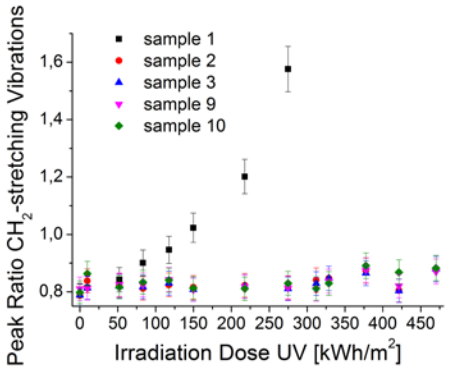

Figure 12: Ratio of the asymmetric to the symmetric stretching vibration of all samples during aging.

For polyethylene Abbate et al. theoretically related the symmetric CH_2 stretching vibration at 2832 cm^{-1} to molecules in trans-conformation and the asymmetric vibration at 2913 cm^{-1} to molecules in gauche-conformation. The trans-conformation is an energetically more stable conformation and crystals are therefore always based on molecules in trans-conformation. Accordingly Abbate et al. experimentally observed, that the relative change of ratio from trans- to gauche-conformation corresponds to a decreasing crystallinity of polyethylene [8]. Therefore the observed change of ratio could be explained by a conformational change of the polyethylene molecules from trans-conformation to gauche-conformation during aging. This could possibly be accompanied by a relative decrease in crystallinity. Furthermore changes to gauche-conformations are possibly connected to defects and changes in mechanical properties.[9] This could be one of the reasons for the observed crack development.

3.3 DSC measurements

In order to relate the significant conformational changes in sample 1 to changes in crystal structure DSC measurements were conducted.

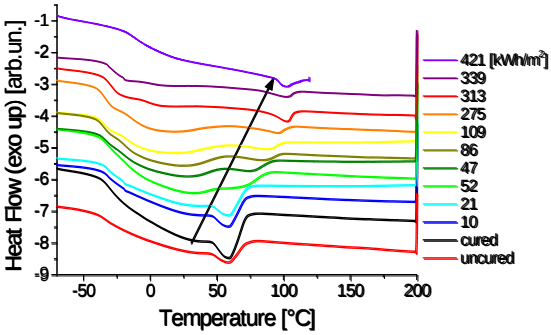

Figure 13: DSC thermograms during aging (2nd cycles).

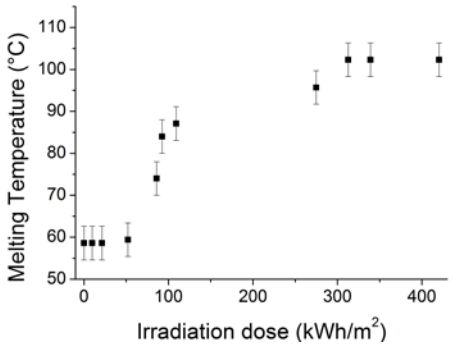

Figure 14: Evolution of the highest temperature endothermal peak according to DSC of sample 1.

Figure 13 shows the second DSC cycle between -80 ° to 200 °C for sample 1. The second cycle is taken for evaluation to exclude thermal influences. The endothermic peak derives from crystal melting. As can be seen in Figure 14 the melting temperature increases during the aging process. Higher melting temperatures indicate a more organized crystal phase. [10] This corresponds to the increase of the CH_2 scissoring vibration at 1416 cm^{-1}, which also indicates the development of an increasingly organized crystal phase during aging. This might also be correlated with thicker crystal lamellae. In this case, a higher tension weights on the tie-molecules that connect the crystal domains.[10] This could also have contributed to the observed crack development. Again it is important to note, that only a conclusion about the amount of highly organized crystals can be drawn from these results. The development of the total amount of crystals might be different.

3.4 UV-vis spectroscopy

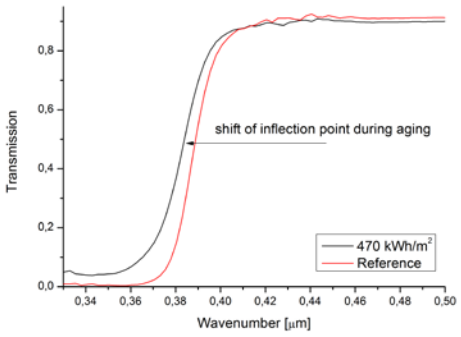

Figure 15:UV-vis spectrum of tha unaged and aged sample 10

UV absorbers determine the UV cutoff. Cyabsorb 531 (sample 10, 350 nm) shows the lowest UV cutoff. Samples 2, 3, and 9 all contain Tinuvin 234, they show slightly different cutoffs (sample 2 and 10: 360 nm; sample 3: 370 nm). This might either be due to variations in the UV absorber concentration or to a synergistic reaction of Irgafos 168 and Tinuvin 770.
If the UV absorbers lose their UV absorbing property due to degradation, the inflection point of the spectrum shifts to lower wavelengths and a greater amount of UV light is transmitted (Figure 15). In order to follow the degradation of the UV absorbers, the UV-vis

transmission spectra were integrated between 340 nm (zero transmission) and the inflection point (Figure 16).

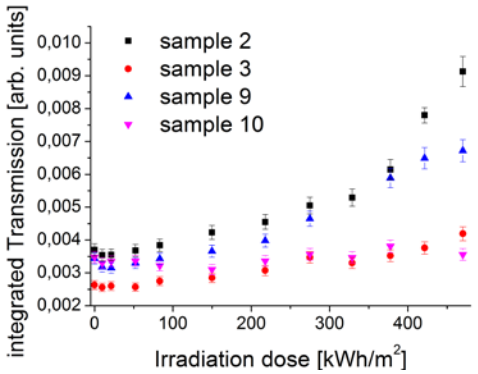

Figure 16: UV transmission integrated between 340 nm and the inflection point.

The transmission in the UV range of sample 2 and 9 (Tinuvin 234) increases significantly more than it does for sample 3 (Tinuvin 234) and sample 10 (Cyabsorb 531). This indicates a higher stability of Cyabsorb 531. Because free standing films were used, it is also possible that Tinuvin 234 is more easily volatilized or otherwise lost. Sample 3 contains the same composition like sample 9 with the exception of the antioxidant Irgafos 168. Therefore Irgafos 168 might protect Tinuvin 234 from decomposition. But the lower loss of the UV absorber in sample 3 might also be correlated to the higher UV cutoff of sample 3.

Furthermore the Solar Transmittance (AM1,5) was determined (Figure 17). Due to the fast degradation of sample 1, UV-vis measurements of sample 1 were only possible up to 80 kWh/m^2. There is a significant trend towards a decrease in Solar Transmittance for all the samples with added stabilizers. This is most likely related to the development of chromophoric species. It can either derive from common degradation products or is caused by additive interactions. In particular their photolysis in the presence of peroxide is a possible origin.[4] As all samples show a similar total decrease, the development cannot directly be related to specific additive interactions.

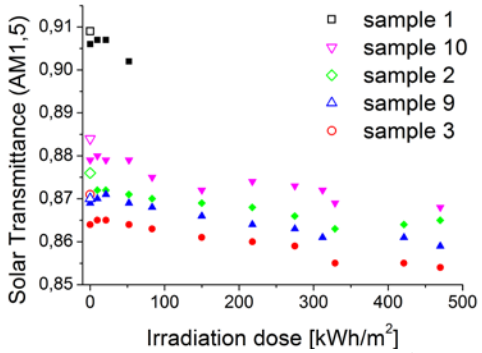

Figure 17: The Solar Transmittance (AM1,5) for all samples during aging. The non-filled points are the uncured samples.

The Solar Transmittance of sample 1 is ca. 3 % higher than for the other samples. This is presumably mainly due to the higher UV cutoff in the samples with added stabilizers. This also explains the higher solar transmittance of the sample 10. Curing also causes a drop in solar transmittance possibly because of curing generated chromophoric species.[1]

4 DISCUSSION

4.1 Degradation of the sample without added stabilizers

Changes in the carbonyl region of the Raman spectrum and the development of C=C bounds indicate, that sample 1 degraded via deacetylation accompanied by ketone and lactone formation. This is in accordance with former observations.[2]

During aging we saw a reduction of the Raman intensity of all PE related peaks, an increase of the carbonyl peak and the liquefaction of sample 1.[2] All of these effects are an expected result of chain scission. Deacetylation and chain scission facilitate chain diffusion processes, which might lead to the development of better organized crystals as indicated by the increase of Raman intensity of the CH_2 scissoring vibration at 1416 cm^{-1} and the increasing crystalline melting temperature. Despite of the relative increase of better organized crystals, the change in ratio of the symmetric to the asymmetric CH_2 stretching vibrations indicates a relative decrease of crystalline structure.[8] It also suggests a relative increase of molecules in gauche-conformation.[8] This might be connected with the introduction of defects and contribute to the observed cracking.[9] A possible explanation for the hardening could be the development of radical induced crosslinks like it has been observed previously.[1]

4.2 Degradation of the samples with stabilizers

The samples show a pronounced development of fluorescent species, with significant differences. Therefore it is likely to be the result of additive interactions. In particular the combination of Tinuvin 234 (UV-absorber) and Tinuvin 770 (HALS) might support the development of fluorescent species or conversely, might not hinder their destruction. Compared to samples, that were aged in a glass-EVA-glass setup the development of fluorescence is significantly smaller, which might be the effect of oxygen induced quenching.[12] The samples with stabilizers show 1-3 % lower solar transmittance than sample 1, attributable to UV absorbers and to a lesser extent on the formation of chromophoric species.[11] The total solar transmittance is reduced by ca. 1 % during aging for all samples with added stabilizers. Due to the loss of UV absorber properties, the UV cutoffs shift to lower wavelengths during aging. The sample with Cyabsorb 531 (sample 10) showed a smaller shift and therefore Cyabsorb 531 seems to be more stable than Tinuvin 234 (sample 2, 3, 9) despite its lower UV cutoff. It is possible that Tinuvin 234 is more easily lost from the free standing films. Irgafos 168 (antioxidant) and Tinuvin 234 (sample 3) might react synergistically to reduce Tinuvin 234 decomposition.

4.3 Nondestructive analytical methods for EVA degradation

Regarding non-destructive analytical methods for monitoring degradation Raman spectroscopy proved itself to be a very useful method. In particular the detection of the ratio of the symmetric to the asymmetric

CH_2 stretching vibrations seems to be a promising method regarding the detection of conformational changes as well as changes in the crystal ratio. A great advantage of the CH_2 stretching vibration is their high peak intensity, which makes them detectable at higher fluorescence intensities.
Additionally it was observed that crosslinking reduces the intensity of all investigated polyethylene related peaks, possibly because the free chain length between crosslinks is reduced. This could provide a non-destructive method to evaluate the crosslinking degree in EVA.

5 CONCLUSION

The sample 1 without stabilizers first became fluid, then hardened and cracked in the course of aging. The samples with stabilizers only showed the development of chromophoric and fluorescent species as well as the consumption of the UV absorbers. Sample 1 most likely degraded via deacetylation accompanied by ketone and lactone formation as well as chain scission. Both processes support the development of better organized crystals, which were observed by Raman spectroscopy and DSC. Despite the increase of better organized crystals the relative increase of the amount of molecules in gauche conformation indicates, that the total amount of crystals most likely decreases and the number of defects increases. This might have contributed to the observed crack development. Chain scission is a likely reason for the observed liquefaction of sample 1, whereas radical induced crosslinks might have contributed to the hardening.
Additives most likely enhance the development of fluorescent species in the samples with added stabilizers. Oxygen most likely reduces this effect due to photobleaching. The UV absorber Cyabsorb 531 appeared to be more stable than Tinuvin 234. A possible synergy between Irgafos 168 and Tinuvin 770 was observed. The combination of Tinuvin 234 (UV-absorber) and Tinuvin 770 (HALS) might enhance the development fluorescent species or reduce the rate of fluorophore decomposition.

References

1. Czanderna, A.W. and F.J. Pern, *Encapsulation of PV modules using ethylene vinyl acetate copolymer as a pottant: A critical review.* Solar Energy Materials and Solar Cells, 1996. **43**(2): p. 101-181.
2. Rodríguez-Vázquez, M., et al., *Degradation and stabilisation of poly(ethylene-stat-vinyl acetate): 1 – Spectroscopic and rheological examination of thermal and thermo-oxidative degradation mechanisms.* Polymer Degradation and Stability, 2006. **91**(1): p. 154-164.
3. Pern, F.J., *Ethylene-vinyl acetate (EVA) encapsulants for photovoltaic modules: Degradation and discoloration mechanisms and formulation modifications for improved photostability.* Die Angewandte Makromolekulare Chemie, 1997. **252**(1): p. 195-216.
4. Klemchuk, P., et al., *Investigation of the degradation and stabilization of EVA-based encapsulant in field-aged solar energy modules.* Polymer Degradation and Stability, 1997. **55**(3): p. 347-365.
5. Peike, C., et al., *Towards the Origin of EVA Discoloration in PV Modules*.
6. Zavgorodnev, Y.V., et al., *Raman structural study of reactor blends of ultrahigh molecular weight polyethylene and random ethylene/1-hexene copolymers.* Laser Physics, 2013. **23**(2): p. 025701.
7. Strobl, G., *The Physics of Polymers*. 1997, Heidelberg Berlin: Springer Verlag.
8. Abbate, S.Z., G., *Fermi Resonaces and Vibrational Spectra of Crystalline and Amorphous Polymethylene Chains.* The Journal of Physical Chemistry, 1982. **86**(16): p. 3140-3149.
9. Špitalský, Z. and T. Bleha, *Elastic moduli of highly stretched tie molecules in solid polyethylene.* Polymer, 2003. **44**(5): p. 1603-1611.
10. Ehrenstein, G., *Polymer Werkstoffe*. 2011, München: Carl-Hanser Verlag.
11. Pern, F.J., *Ethylene-vinyl acetate (EVA) encapsulants for photovoltaic modules: Degradation and discoloration mechanisms and formulation modifications for improved photostability.* Die Angewandte Makromolekulare Chemie, 1997. **252**: p. 195-216.
12. Peike, C., et al. *Towards the origin of photochemical EVA discoloration*. in *Photovoltaic Specialists Conference (PVSC), 2013 IEEE 39th*. 2013.